coatings

MDPI

Article

Comparative Evaluation of Coated Carbide and CBN Inserts Performance in Dry Hard-Turning of AISI 4140 Steel Using Taguchi-Based Grey Relation Analysis

Mustafa Özdemir [1], Mohammad Rafighi [2,*] and Mohammed Al Awadh [3]

[1] Department of Machine and Metal Technology, Yozgat Bozok University, Yozgat 66200, Türkiye; mustafaozdemir58@gmail.com
[2] Department of Mechanical Engineering, Başkent University, Ankara 06790, Türkiye
[3] Department of Industrial Engineering, King Khalid University, Abha 61411, Saudi Arabia; mohalawadh@kku.edu.sa
* Correspondence: mohammad.rafighi@gmail.com

Abstract: Dry hard-turning is a vital manufacturing method for machining hardened steel due to its low cost, high machining efficiency, and green environmental protection. This study aims to analyze the effect of various machining parameters on cutting forces and surface roughness by employing RSM and ANOVA. In addition, multi-objective optimization (Grey Relation Analysis: GRA) is performed to determine the optimum machining parameters. Dry hard-turning tests were carried out on AISI 4140 steel (50 HRC) using coated carbide and CBN inserts with different nose radii. The results show that the cutting force components are greatly affected by the cutting depth and cutting speed for both cutting inserts. As the level of cutting depth and cutting speed rise, the cutting forces also increase. However, the feed rate was the main factor in surface roughness. A low feed rate and high cutting speed lead to good surface quality. According to the results, CBN inserts exhibited better performance compared to carbide inserts in terms of minimum cutting forces and surface roughness. The lowest radial force (Fx = 55.59 N), tangential force (Fy = 15.09 N), cutting force (Fz = 30.49 N), and best surface quality (Ra = 0.28 µm, Rz = 1.8 µm) were obtained using a CBN tool. Finally, based on the GRA, the (V = 120 m/min, f = 0.04 mm/rev, a = 0.06 mm, r = 0.8 mm) have been chosen as optimum machining parameters to minimize all responses simultaneously in the machining of AISI 4140 steel using both carbide and CBN inserts.

Keywords: dry hard-turning; surface roughness; cutting forces; optimization; grey relation analysis

Citation: Özdemir, M.; Rafighi, M.; Al Awadh, M. Comparative Evaluation of Coated Carbide and CBN Inserts Performance in Dry Hard-Turning of AISI 4140 Steel Using Taguchi-Based Grey Relation Analysis. *Coatings* **2023**, *13*, 979. https://doi.org/10.3390/coatings13060979

Academic Editors: Yuxin Wang, Filipe Daniel Fernandes, Hongbo Ju and Bingyang Ma

Received: 27 April 2023
Revised: 17 May 2023
Accepted: 22 May 2023
Published: 24 May 2023

1. Introduction

Many manufacturers aim to produce the maximum amount of product in the minimum amount of time without compromising the quality of the product [1]. In this context, environmentally friendly hard-turning, which provides significant benefits such as flexibility in operation, lower setup and cycle times, lower operating costs, and less power and energy consumption, is a selectable process. Hard-turning is performed on materials having 40 to 65 HRC (Rockwell Hardness) [2]. The grinding process is an alternative to hard turning. However, hard-turning is more popular than the grinding process due to its high stock removal ability and capacity to produce complex geometries. In addition, it has been shown to be an environmentally friendly process since no cutting fluid is used in dry hard-turning [3–5].

Heat-treated steels have a wide range of applications in the aerospace and automotive industries, but the finishing process for such steels is challenging and expensive. Nowadays, the turning of hardened steel is possible thanks to advances in tool material and coating technology. Hardened steel is carbon steel composed of approximately 2.1% carbon. In addition, the hardened steel can be subjected to different heat treatment processes to achieve

the desired hardness [6]. Hardened steels are widely used in the aerospace, automotive, and machine tool manufacturing industries due to their excellent properties, such as high wear resistance, corrosion resistance, and durability [7]. It is desired to produce machine parts with high tolerances, high dimensional accuracy, and superior surface quality in the aerospace and automotive industries [8]. The most widely used steel is quenched and tempered AISI 4140 steel, used in the manufacturing and automotive industries. It is widely used in the manufacture of mechanical parts such as shafts, gears, and balls [9]. Cubic Boron Nitride (CBN) is a suitable cutting tool for machining hardened steels, exhibiting high toughness, hardness, and a stable structure at high temperatures [10]. On the other hand, high tool costs and machinability limitations are the problems that stand in the way of the hard-turning process [11]. PCBN (Polycrystalline Cubic Boron Nitride) and diamond inserts have high production costs and limited stocks. Therefore, it is necessary to choose a good solution in terms of performance and quality.

Surface quality is one of the most crucial points of the hard-turning process. Recent studies show that workpiece/cutting tool characteristics affect surface quality. Therefore, it is imperative to investigate the relationship between workpiece/tool properties and surface quality [12]. Another important factor influencing the hard-turning process is tool geometry. Surface quality, tool wear, heat generation, chip formation, and cutting force are greatly affected by tool geometry [13,14]. The most important step following the material and cutting tool is the selection of proper machining parameters. Cutting speed, feed rate, and cutting depth should be determined according to the material and cutting tool. High temperatures and cutting forces are generated during hard turning [15]. Therefore, reducing the cutting force is another critical point in hard turning. Recent studies on turning AISI 4140 steel are presented below, and the results are analyzed comprehensively. So far, no experimental study has been conducted to compare CBN and carbide tools in dry hard-turning in terms of both cutting force and surface roughness. In the current study, the effects of machining parameters, tool types (CBN and carbide), and geometries on the cutting forces and surface roughness are investigated in hard-turning AISI 4140 steel.

Gürbüz and Gönülaçar [9] used carbide inserts in hard turning of AISI 4140 steel under MQL and dry cutting conditions. They reported that Fc and Ra increased with increasing feed rates, and Fc tended to decrease with increasing shear rates. MQL application reduced Fc and Ra overall compared to dry machining, and Ra increased with increasing feed rate. The minimum Ra is recorded as 1.090 µm for the MQL condition.

Schwalm et al. [14] examined the effect of different tool types, machining parameters, and lubrication strategies on the resulting roughness and tool wear. Based on the results, tool type has an influential effect on surface roughness. The type I PVD-coated carbide tool results in a minimum surface roughness of 0.55 µm.

Tool life, cutting forces, and tool wear mechanisms were analyzed for surface roughness in the Nikam et al. [16] study. The machining forces increased as the input variables increased. Besides, increasing the feed rate augmented surface roughness. The minimum surface roughness was measured at 0.518 µm.

Aouici et al. [17] compared different ceramic inserts, considering cutting force and flank wear. The results revealed the dominant effect of cutting depth on the cutting force components. Generally, CC650WG and CC650 ceramic inserts produce lower cutting forces compared to others. The minimum cutting force (Fx) was recorded as 14.07 N for the CC650WG insert.

According to many studies on AISI 4140 steel, the feed rate was the most significant indicator of surface roughness. Increasing the feed rate sharply enhances surface roughness [18–20].

Upadhyay [21] used Grey Relational Analysis to optimize surface roughness, cutting force, and material removal rate (MRR) based on different machining parameters. According to the results of GRA, the optimum machining parameter combination was found to be 0.8 mm cutting depth, 180 m/min cutting speed, and 0.15 mm/rev feed rate. In addi-

tion, the feed rate was determined to be the most influential parameter on the responses, followed by cutting speed. The minimum Rz was recorded as 0.359 µm.

Elbah et al. [22] studied the performances of the machining environments (dry, conventional wet, and MQL technique) in terms of surface roughness and cutting force. It was stated that the cutting force obtained with the MQL machining process improved significantly when compared to other machining processes. The minimum surface roughness was obtained using dry machining (0.21), followed by MQL machining (0.23). However, the mean surface roughness for all combinations of machining parameters in wet and MQL machining is better than in dry machining.

Tiwari et al. [23] investigated the applicability of solid lubricants considering different conditions, namely, dry, flood cooling, grease, and MoS2. The surface quality improved when using solid lubricants such as grease and MoS2.

Sultana et al. [24] reported that the effects of process parameters on roughness, cutting force, specific cutting energy requirements, and material removal rate (MRR) were investigated using LN2-assisted cryogenic cooling. The performance of LN2-assisted cryogenic turning outperformed without coolant machining in terms of roughness, principal force, and specific cutting energy. Generally, the feed rate was considered the most significant factor in the responses. However, according to the Taguchi-linked GRA, the cutting environment was the most dominant factor, followed by the feed rate.

Nicolodi et al. [25] presented the effect of tool wear on machining forces and surface roughness. The findings show that a high feed rate and cutting speed significantly affect both flank and crater tool wear, and the feed rate was the dominant parameter on surface roughness and machining force.

Meddour et al. [26] studied the impact of tool nose radius, cutting depth, cutting speed, and feed rate on surface roughness and cutting forces. A combination of a large nose radius and a low feed rate results in good surface quality. However, the cutting forces (Fx, Fy, and Fz) are significantly impacted by cutting depth. The minimum surface roughness is measured as 0.24 µm and the minimum Fx is recorded as 17.94 N for a 0.8 mm nose radius.

Zahia et al. [27] also reported the same results regarding the impact of feed rate and cutting depth on surface roughness and cutting forces, respectively.

According to most studies [28–31], it has been concluded that the most important factor in surface roughness is feed rate. However, Akkuş [32] stated that the cutting depth is the most important factor in Ra. On the other hand, Bagal et al. [33] stated that both cutting speed and cutting depth were the most effective parameters for surface roughness, while feed rate was the least effective.

By analyzing the literature, the lowest surface roughness (0.1 µm) is obtained with the ceramic tool (V = 180 m/min, f = 0.08 mm/rev, a = 0.2 mm) [34], while the minimum Ra values for CBN tools (0.17 µm) were obtained when using a 0.8 mm corner radius [35]. The least surface roughness (0.2 µm) value for carbide inserts was obtained with a combination of V = 190 m/min, f = 0.05 mm/rev, and a = 0.05 mm machining parameters [36]. In the presented study, the performance of CBN and coated carbide inserts is compared in terms of minimum surface roughness and cutting forces. The lowest surface roughness for a CBN insert is (0.28 µm) and for a carbide insert is (0.35 µm) with a combination of (V = 180 m/min, f = 0.04 mm/rev, a = 0.18 mm, r = 0.8 mm) which are close to the obtained results in the literature survey. In the previous studies, the minimum cutting force for carbide inserts was calculated as 15.33 N (V = 170 m/min, f = 0.08 mm/rev, a = 0.3 mm) [37]. In this study, the cutting force values for carbide and CBN inserts were calculated as 15.09 N and 25.06 N, respectively, which are in good agreement with the literature survey. Generally, high cutting speed and low feed rate lead to minimum surface roughness, while low cutting depth and cutting speed result in minimum cutting force.

2. Materials and Methods

In this study, AISI 4140 alloy steel was used as a material for the machining tests. Appropriate heat treatments have been carried out to achieve a hardness of 50 HRC. The

cylindrical material is 40 mm in diameter and 240 mm in length. A thermo-scientific X-ray fluorescence spectrometer was used to determine the chemical composition of the test workpiece. The chemical composition, thermal, and mechanical properties of AISI 4140 steel are given in Table 1.

Table 1. Chemical composition, mechanical, and thermal properties of AISI 4140 steel.

Chemical Composition (wt. %)						
C	**Si**	**Mn**	**Cr**	**Mo**	**Fe**	
0.38–0.43	0.15–0.3	0.7–1	0.8–1.1	0.15–0.25	Balance	
Mechanical and thermal properties						
Density	**Young's modulus (at 25 °C)**	**Poisson's ratio (at 25 °C)**	**Tensile strength**	**Yield strength**	**Specific heat (at 25 °C)**	**Thermal conductivity (at 25 °C)**
7850 kg/m^3	198 GPa	0.3	729.5 MPa	379.2 MPa	470 j/kg°C	42.7 W/m°C

Hard-turning experiments were carried out on the GoodWay GS-260Y CNC lathe using variable cutting speeds, feed, depths of cut, and tool nose radii. Since dry cutting conditions are considered an environmentally friendly process, all experiments were performed without the use of cutting fluid [2–5]. Dry cutting conditions are not only an environmentally friendly process but also economically affordable by neglecting the costs of purchasing and disposing of cutting fluids [38]. Hard-turning is usually performed with PCBN or mixed ceramic tools that are even harder than the machined material and can withstand the tribological conditions of the process [39]. Cubic boron nitride (CBN) tool material, which exhibits high toughness, high hardness, and a stable structure at high temperatures, is suitable for hardened steels. It has been stated that the CBN cutting tool performs better than coated carbide tools in terms of tool wear and surface quality [40,41]. In this study, the performance of the coated carbide (CNMG120404-MK5 WKK10S) and CBN (CNMA 433-2 WCB50) inserts was compared in addition to the effect of machining parameters and cutting conditions on the surface roughness and cutting forces. The experimental setup is given in Figure 1.

Taguchi L9 experimental design was used to determine the effect of machining parameters shown in Table 2 on surface roughness and cutting forces. In this regard, nine experiments were performed for each insert instead of 81 to evaluate the results. Response surface methodology was used in MINITAB 20 software to analyze the effect ratios of machining parameters. Besides, the percentage contribution of each machining parameter to the response variables was examined using ANOVA. Finally, regression analysis established mathematical models for each cutting insert.

Table 2. Machining parameters for hard-turning AISI 4140 steel.

Factor	Level 1	Level 2	Level 3
Cutting insert	Carbide	CBN	-
Cutting speed (m/min)	120	150	180
Feed rate (mm/rev)	0.04	0.08	0.12
Cutting depth (mm)	0.06	0.12	0.18
Nose radius (mm)	0.4	0.8	1.2

The 9129AA-type Kistler force dynamometer was used to measure the force signals during the cutting process. Ra and Rz roughness parameters were measured using the Mitutoyo SJ-400 surface roughness tester. Average surface roughness was measured according to the ISO-4288:2011 standard [42]. The arithmetic height means Ra is one of the most widely accepted measurements for surface roughness. It is a good and practical indicator to evaluate the surface quality. Ra is the mean of the absolute height deviation from the mean line along the sampling length. The 10-point roughness parameter Rz was also used in the present study, as it is more sensitive than Ra to the irregular heights or depths of peaks and valleys. According to the international ISO standard, Rz is the difference between the five

maximum peaks' mean and the five minimum valleys along the measured length [43]. The raw material's surface roughness was measured at 3.07 µm.

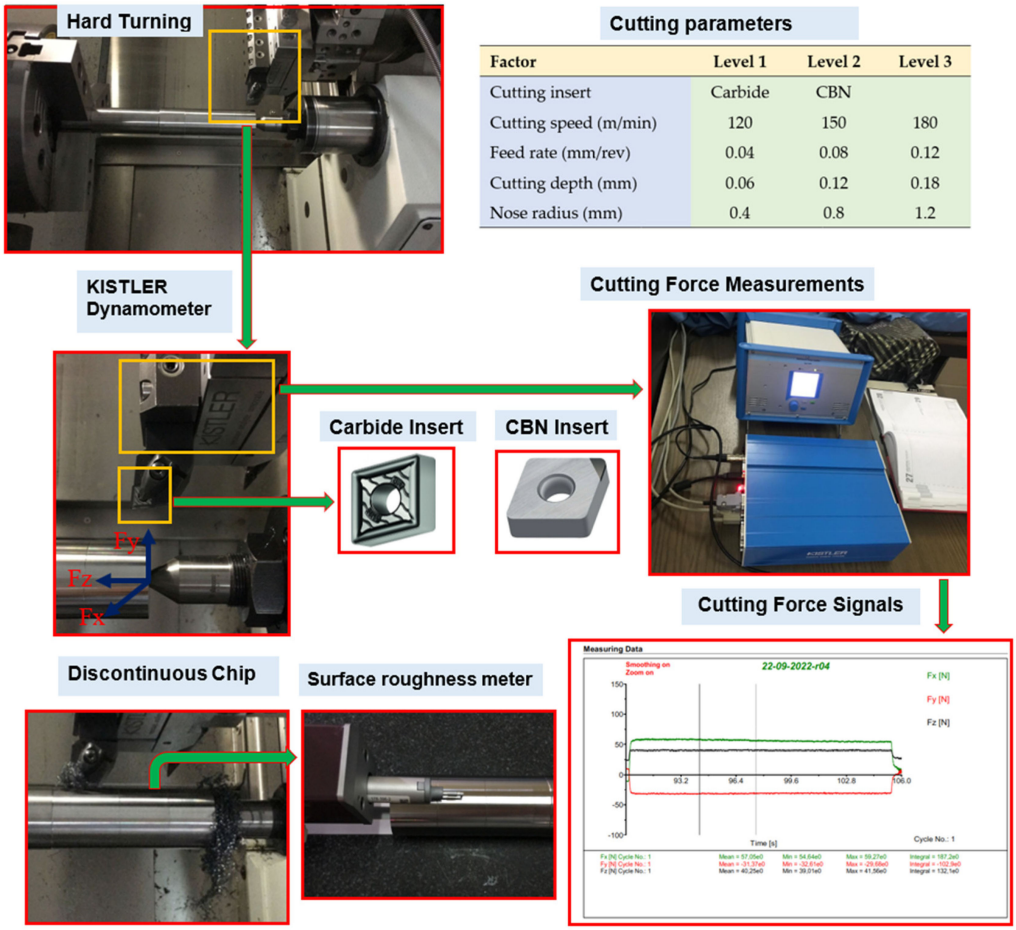

Factor	Level 1	Level 2	Level 3
Cutting insert	Carbide	CBN	
Cutting speed (m/min)	120	150	180
Feed rate (mm/rev)	0.04	0.08	0.12
Cutting depth (mm)	0.06	0.12	0.18
Nose radius (mm)	0.4	0.8	1.2

Figure 1. Experimental setup of the turning process.

3. Results and Discussion

The experimental results during dry hard-turning of AISI 4140 steel using carbide and CBN inserts are given in Table 3. This table presents the measured surface roughness parameters (Ra and Rz) and the measured cutting force components (Fx, Fy, and Fz). Here Fx is the radial force, Fy is the tangential force, and Fz is the cutting force.

The raw material's surface roughness was measured at 3.07 µm. However, after the hard-turning process, Ra for carbide inserts is recorded in the range of 0.35 µm and 0.63 µm, while for CBN inserts it is 0.28 µm and 0.59 µm. Rz for carbide inserts varies between 2.4 µm and 4.4 µm, while for CBN inserts it varies between 1.8 µm and 3.8 µm. The cutting force components for the carbide insert are 25.06–198.56 N, while for the CBN insert, they are 15.09–94.36 N. The results showed that the cutting force components are very sensitive to the cutting depth, whereas the surface roughness is greatly affected by feed rate. The feed and cutting depth are functions of the chip cross-sectional area. Thus, as the feed increases, the chip area (undeformed chip thickness) in the machining area augments, which results in a higher cutting force and surface roughness [16].

Tool material is another important factor affecting cutting force. There was a significant reduction in cutting forces using the CBN tool. In terms of radial force (Fx), tangential force (Fy), and cutting force (Fz), the CBN insert presented, respectively, 103%, 62%, and 40% better performance (lower cutting forces) than the carbide inserts. In addition, it was observed that the mean surface roughness for CBN inserts (0.427 µm) is 14% lower than for carbide inserts (0.485 µm). The next important factor affecting the surface roughness is the cutting speed. Cutting speed is one of the essential controlled machining parameters

for hard turning [44]. Higher cutting speeds increase the cutting force components; on the contrary, the surface roughness drops as the cutting speed rises.

The minimum cutting force components were determined with a CBN tool (V = 120 m/min, f = 0.04 mm/rev, a = 0.06 mm, r = 0.4 mm). Generally, the radial force is greater than the tangential and cutting forces for both cutting inserts. Nikam et al. [16] also stated that the radial force is the highest force component. The possible reason behind the higher radial force generation was the selection of a lower cutting depth than the insert nose radius [45].

Table 3. Cutting forces and surface roughness results for different machining parameters.

Carbide Insert									
NO	**V (m/min)**	**f (mm/rev)**	**a (mm)**	**r (mm)**	**Fx (N)**	**Fy (N)**	**Fz (N)**	**Ra (µm)**	**Rz (µm)**
1	120	0.04	0.06	0.4	111.36	25.06	43.39	0.44	3.1
2	120	0.08	0.12	0.8	129.79	42.98	55.49	0.52	3.6
3	120	0.12	0.18	1.2	151.88	57.25	71.32	0.63	4.4
4	150	0.04	0.12	1.2	150.52	50.67	63.49	0.39	2.7
5	150	0.08	0.18	0.4	174.02	66.69	80.88	0.49	3.5
6	150	0.12	0.06	0.8	126.89	29.46	50.55	0.58	4.1
7	180	0.04	0.18	0.8	198.56	75.97	91.28	0.35	2.4
8	180	0.08	0.06	1.2	141.63	35.69	58.23	0.45	3.1
9	180	0.12	0.12	0.4	172.39	59.78	72.98	0.52	3.6
CBN Insert									
NO	**V (m/min)**	**f (mm/rev)**	**a (mm)**	**r (mm)**	**Fx (N)**	**Fy (N)**	**Fz (N)**	**Ra (µm)**	**Rz (µm)**
1	120	0.04	0.06	0.4	55.59	15.09	30.49	0.39	2.6
2	120	0.08	0.12	0.8	63.78	25.76	38.69	0.46	3.0
3	120	0.12	0.18	1.2	73.59	34.67	50.28	0.59	3.8
4	150	0.04	0.12	1.2	76.09	32.69	45.68	0.33	2.1
5	150	0.08	0.18	0.4	84.67	37.79	65.19	0.44	2.9
6	150	0.12	0.06	0.8	62.87	19.67	36.66	0.51	3.3
7	180	0.04	0.18	0.8	94.36	48.89	61.59	0.28	1.8
8	180	0.08	0.06	1.2	70.56	23.49	41.49	0.40	2.6
9	180	0.12	0.12	0.4	86.01	35.79	50.89	0.45	2.9

3.1. Main Effects Plot and ANOVA Results

Main effect plots showing the effects of cutting speed, feed rate, cutting depth, and tool nose radius on Fx and Ra are given in Figure 2 according to Taguchi's "the lowest is the best" approach. According to the main effects plot, cutting depth and cutting speed have a dominant effect on the Fx, Fy, and Fz for both cutting inserts. As the value of cutting depth and cutting speed augments, the responses also increase sharply due to the removal of large amounts of material from the workpiece. Furthermore, feed rate has a superior impact on Ra and Rz, followed by cutting speed. Increasing the feed rate sharply enhances the surface roughness. In contrast, increasing the cutting speed reduces the surface roughness. It was concluded that the cutting depth and nose radius have a negligible effect on the Ra.

The primary purpose of the analysis of variance is to show which independent variables significantly affect the dependent variables. The ANOVA results for both cutting inserts are given in Table 4, which shows the contribution effect of each machining parameter on the responses. The machining parameters with a *p*-value lower than 0.05 are statistically significant. Due to the negligible effect of factor interactions or squares, only the linear resource is used in the ANOVA analysis. According to the ANOVA results for carbide inserts, cutting depth, with 83.75%, 74.71%, and 58.65% contributions, is the most dominant factor on the Fy, Fz, and Fx, respectively. It was followed by cutting speed with 40.10%, 24.50%, and 14.82% contributions on the Fx, Fz, and Fy, respectively. For a CBN insert, the contribution effect of cutting depth on the Fy, Fz, and Fx is 76.47%, 74.32%, and 53.68%, respectively. It was followed by cutting speed with 44.59%, 20.47%, and 18.91% contributions on the Fx, Fy, and Fz, respectively. Increasing the cutting depth and cutting speed causes higher cutting forces

due to removing a large amount of material. Therefore, a combination of low cutting depth and cutting speed is preferable to reduce the cutting forces.

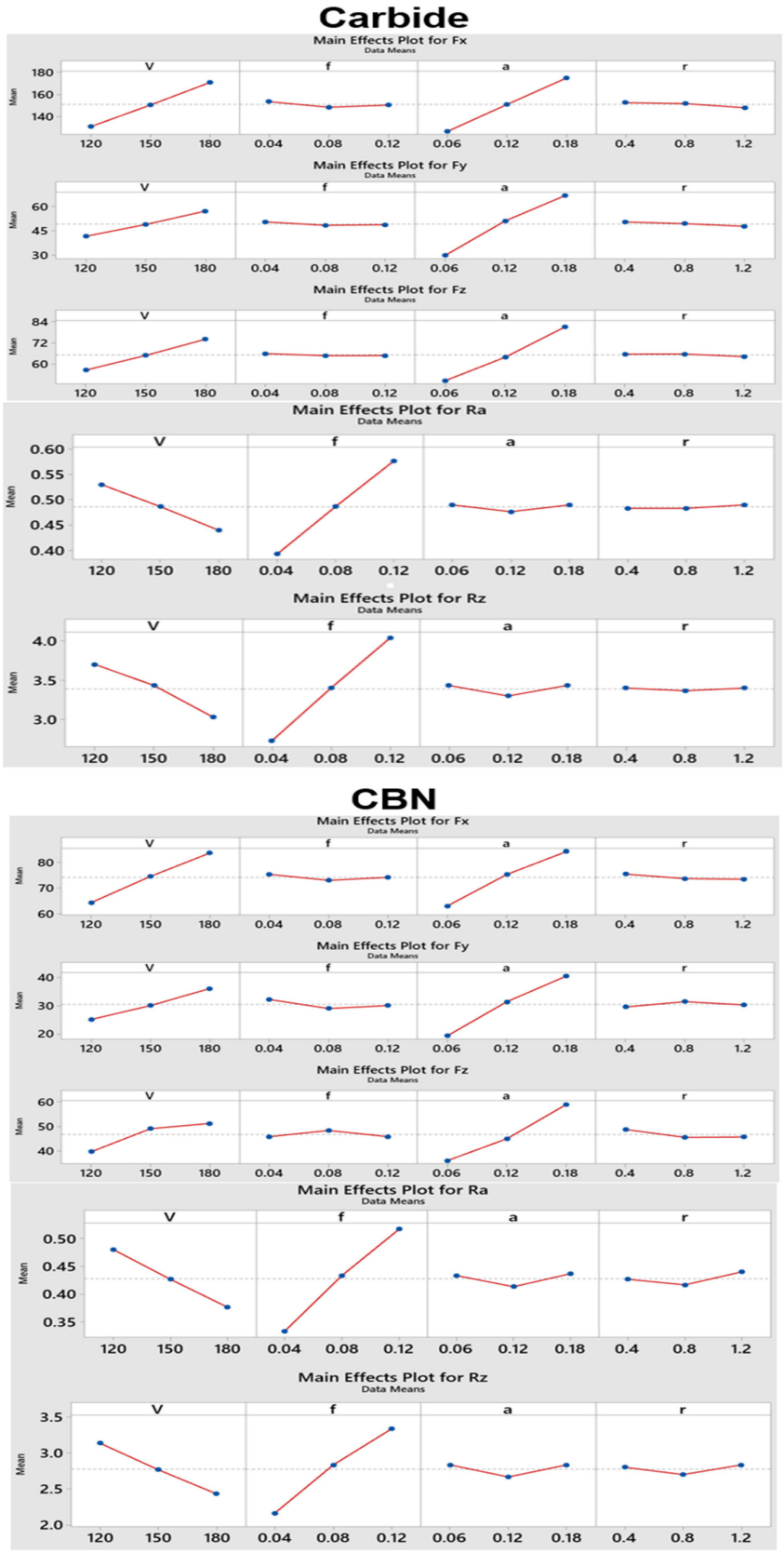

Figure 2. Main effects plot for carbide inserts and CBN inserts.

Table 4. Analysis of variance for cutting forces and surface roughness.

Carbide Insert										
	Fx		Fy		Fz		Ra		Rz	
Source	***p*-Value**	**Cont.**	***p*-Value**	**Cont.**	***p*-Value**	**Cont.**	***p*-Value**	**Cont.**	***p*-Value**	**Cont.**
Linear	0.000	99.52%	0.000	99.19%	0.000	99.46%	0.000	99.38%	0.001	98.55%
V	0.000	40.10%	0.001	14.82%	0.000	24.50%	0.000	19.28%	0.002	20.52%
f	0.229	0.24%	0.388	0.19%	0.440	0.10%	0.000	80.00%	0.000	78.03%
a	0.000	58.65%	0.000	83.75%	0.000	74.71%	1.000	0.00%	1.000	0.00%
r	0.104	0.53%	0.216	0.44%	0.337	0.16%	0.454	0.11%	1.000	0.00%
Error		0.48%		0.81%		0.54%		0.62%		1.45%
Total		100.00%		100.00%		100.00%		100.00%		100.00%
CBN Insert										
	Fx		**Fy**		**Fz**		**Ra**		**Rz**	
Source	***p*-Value**	**Cont.**	***p*-Value**	**Cont.**	***p*-Value**	**Cont.**	***p*-Value**	**Cont.**	***p*-Value**	**Cont.**
Linear	0.000	98.92%	0.001	97.85%	0.009	94.55%	0.002	97.60%	0.003	96.62%
V	0.000	44.59%	0.003	20.47%	0.020	18.91%	0.003	23.43%	0.005	25.56%
f	0.473	0.17%	0.284	0.82%	0.994	0.00%	0.000	73.76%	0.001	71.00%
a	0.000	53.68%	0.000	76.47%	0.002	74.32%	0.850	0.02%	1.000	0.00%
r	0.252	0.48%	0.701	0.09%	0.381	1.32%	0.465	0.39%	0.806	0.06%
Error		1.08%		2.15%		5.45%		2.40%		3.38%
Total		100.00%		100.00%		100.00%		100.00%		100.00%

The feed rate is the dominant factor in the surface roughness of the carbide insert, with 80% and 78.03% contribution effects for Ra and Rz, respectively. Cutting speed is also a significant indicator of the surface roughness for carbide inserts, with contribution effects of 19.28% and 20.52% for Ra and Rz, respectively. For the CBN insert, the impact of feed rate on the Ra and Rz was 73.76% and 71%, respectively. However, the contribution effect of cutting speed on Ra and Rz is 23.43% and 25.56%, respectively. Increasing the feed rate enlarges the chip area in the turned workpiece, which leads to higher surface roughness. In addition, low cutting speed causes the formation of built-up edges (BUE) on the cutting tool that deteriorate surface quality. Therefore, a combination of a low feed rate and a high cutting speed should be chosen to obtain good surface quality.

3.2. Surface Graphs

The 3D surface plot for carbide and CBN inserts considering the interaction of V-a, which is dominant on the cutting force components, is presented in Figure 3, and the 3-D surface plot for surface roughness based on the interaction of V-f is depicted in Figure 4. The cutting force components increase significantly as the cutting depth level is augmented using both cutting inserts. Cutting speed is the next influential factor in the cutting forces. Similarly, as the cutting speed rises, the Fx, Fy, and Fz also enhance. Most of the researchers obtained the same results, indicating the maximum impact of cutting depth on the cutting forces [46,47].

Aouici et al. [17] reported the considerable effect of cutting depth on the cutting force components in the hard-turning of AISI 4140 steel using different ceramic inserts. Tzotzis et al. [47] stated that the dominant effect of cutting depth on the cutting force. İynen et al. [46] also reported the dominant effect of cutting depth on the radial force. Zahia et al. [27] showed the remarkable effect of cutting depth on cutting forces. Increasing the cutting depth sharply enhances the cutting forces.

According to the 3-D surface graph, surface roughness increases using both cutting inserts as the feed rate leads, whereas it decreases as the cutting speed rises. Especially with a combination of low cutting speed and a high feed rate, Ra and Rz increase sharply. High friction occurs between the cutting tool and workpiece at low cutting speeds, reducing surface quality. The minimum surface roughness was obtained using high cutting speeds

and a low feed rate. The higher cutting speed increases the cutting zone temperature, which leads to the thermal softening of the material, and consequently, easy chip removal from the workpiece results in good surface quality [16]. One of the most important tasks of mass production is the safe and efficient removal of chips, which is difficult when chips are constantly formed. The chip types are changed from continuous to serrated in hard-turning as the cutting speed increases, which results in significant waviness and roughness of the machined surface. The significant effect of the feed rate on the surface roughness was presented in many studies [48,49].

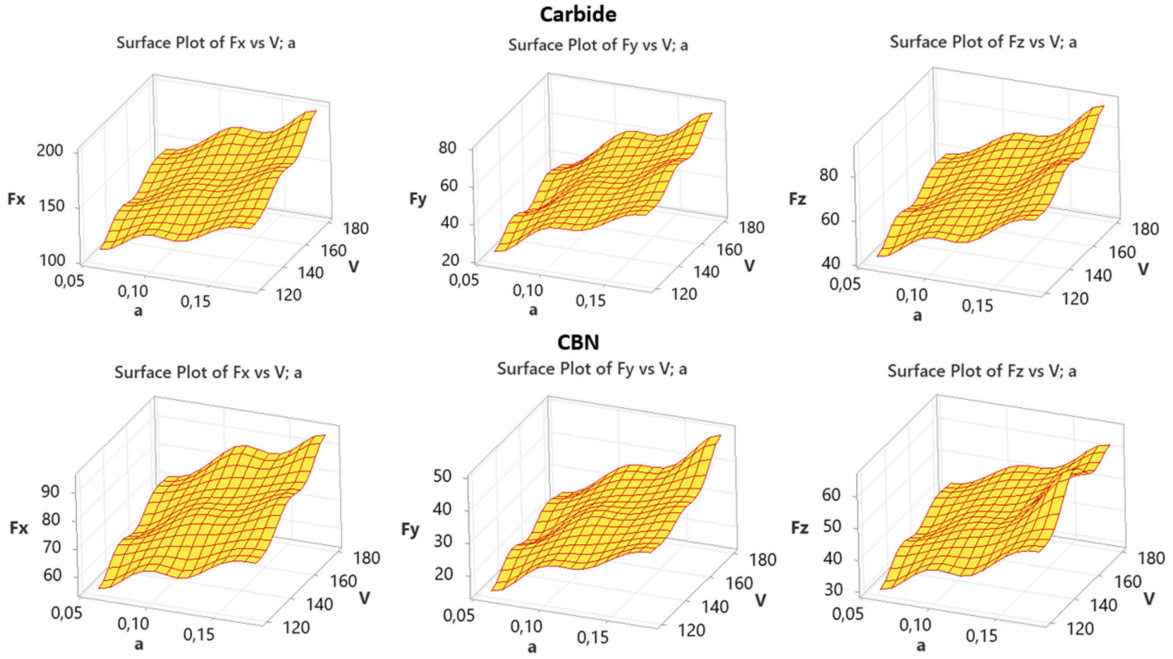

Figure 3. 3-D Surface plot for cutting force components.

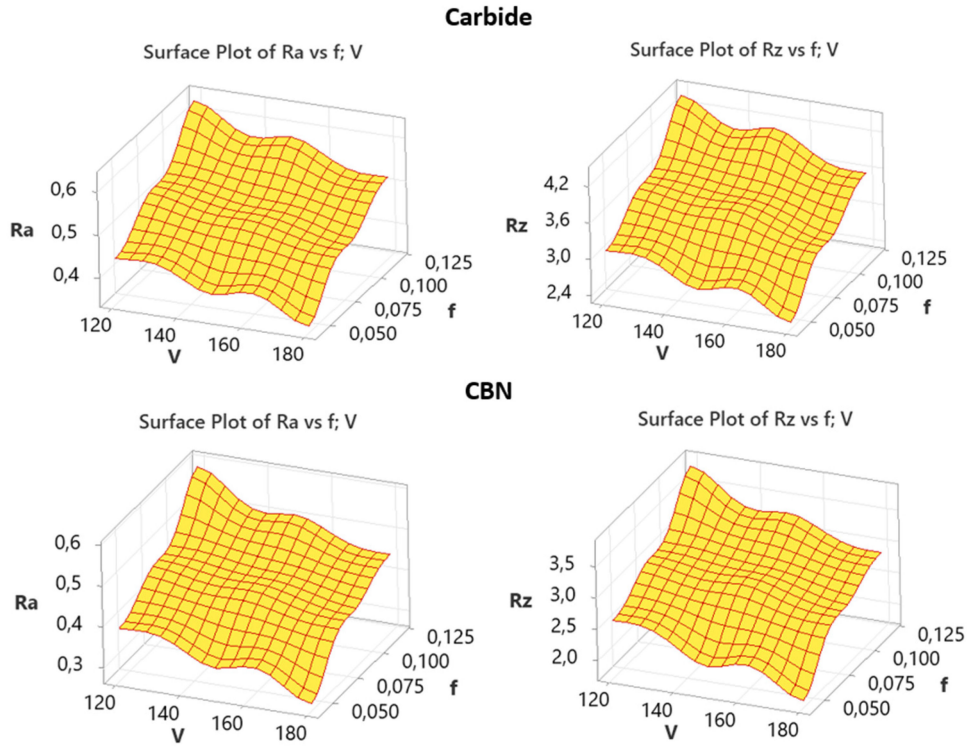

Figure 4. 3-D Surface plot for surface roughness.

İynen et al. [28] stated the dominant effect of feed rate on Ra and Rz. As the feed rate increases, the surface roughness also increases. Mohd et al. [48] reported that the minimum surface roughness was obtained using a low feed rate and high cutting speed. Das [18] and Paengchit [28] also obtained the same results, indicating a dominant effect of feed rate on the surface roughness, followed by cutting speed. Zahia et al. [27] stated the dominant effect of feed rate on surface roughness, followed by cutting speed. They reported that the surface roughness drops as the feed rate decreases and the cutting speed increases. In the presented study, nose radius and cutting depth did not considerably affect the surface quality.

3.3. Prediction Models Using Regression Equations

The multiple regression method was used in this study to develop second-order experimental models at a 95% confidence level for a relationship between machining parameters (V, f, a, r) and output parameters (Fx, Fy, Fz, Ra, Rz) for both cutting inserts. The developed experimental models are given in Equations (1)–(10).

Tool	Regression Equations		R^2	$R^2_{(adj.)}$
Carbide	Fx = 10.64 + 0.6642 V − 38.7 f + 401.6 a − 5.72 r	(1)	99.52%	99.04%
CBN	Fx = 7.86 + 0.3221 V − 14.9 f + 176.7 a − 2.51 r	(2)	*98.92%*	97.84%
Carbide	Fy = −21.37 + 0.2564 V − 21.7 f + 304.7 a − 3.30 r	(3)	99.19%	98.38%
CBN	Fy = −16.36 + 0.1814 V − 27.2 f + 175.3 a + 0.91 r	(4)	97.85%	95.71%
Carbide	Fz = −6.22 + 0.2905 V − 13.8 f + 253.6 a − 1.75 r	(5)	99.46%	98.93%
CBN	Fz = −1.78 + 0.1917 V + 0.3 f + 190.1 a − 3.80 r	(6)	94.55%	89.09%
Carbide	Ra = 0.5206 − 0.001500 V + 2.292 f + 0.000 a + 0.0083 r	(7)	99.38%	98.77%
CBN	Ra = 0.4861 − 0.001722 V + 2.292 f + 0.028 a + 0.0167 r	(8)	97.60%	95.20%
Carbide	Rz = 3.756 − 0.01111 V + 16.25 f + 0.00 a + 0.000 r	(9)	98.55%	97.09%
CBN	Rz = 3.328 − 0.01167 V + 14.58 f + 0.00 a + 0.042 r	(10)	96.62%	93.24%

Experimental results and predicted results using the abovementioned equations for cutting force components and surface roughness are presented in Table 5.

In addition, a graphical comparison of the experimental and predicted results is depicted in Figure 5 for Fx and Ra using both cutting inserts. Clearly, the presented model fits well with the experimental results since the values are very close.

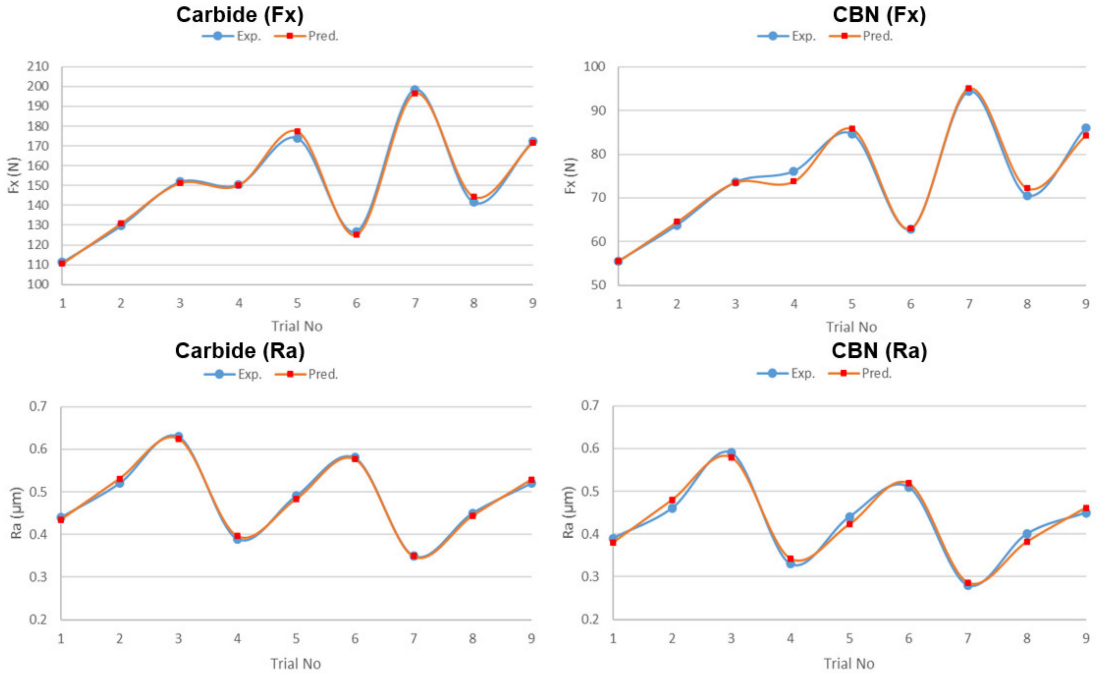

Figure 5. Comparison of experimental and predicted results for Fx and Ra.

Table 5. Experimental and predicted results.

Carbide Insert										
No	**Fx (N)**		**Fy (N)**		**Fz (N)**		**Ra (μm)**		**Rz (μm)**	
	Exp.	**Pred.**	**Exp.**	**Pred.**	**Exp.**	**Pred.**	**Exp.**	**Pred.**	**Exp.**	**Pred.**
1	111.36	110.61	25.06	25.49	43.39	42.61	0.44	0.435	3.1	3.08
2	129.79	130.86	42.98	41.59	55.49	56.57	0.52	0.531	3.6	3.73
3	151.88	151.13	57.25	57.68	71.32	70.53	0.63	0.625	4.4	4.38
4	150.52	150.05	50.67	48.82	63.49	65.13	0.39	0.397	2.7	2.74
5	174.02	177.17	66.69	68.88	80.88	81.20	0.49	0.483	3.5	3.39
6	126.89	125.14	29.46	30.13	50.55	49.52	0.58	0.577	4.1	4.04
7	198.56	196.36	75.97	76.12	91.28	89.77	0.35	0.349	2.4	2.41
8	141.63	144.33	35.69	37.37	58.23	58.09	0.45	0.444	3.1	3.06
9	172.39	171.46	59.78	57.42	72.98	74.15	0.52	0.529	3.6	3.71
CBN Insert										
No	**Fx (N)**		**Fy (N)**		**Fz (N)**		**Ra (μm)**		**Rz (μm)**	
	Exp.	**Pred.**	**Exp.**	**Pred.**	**Exp.**	**Pred.**	**Exp.**	**Pred.**	**Exp.**	**Pred.**
1	55.59	55.52	15.09	15.20	30.49	31.12	0.39	0.379	2.6	2.53
2	63.78	64.51	25.76	25.00	38.69	41.02	0.46	0.479	3.0	3.13
3	73.59	73.52	34.67	34.79	50.28	50.92	0.59	0.579	3.8	3.73
4	76.09	73.77	32.69	31.89	45.68	45.24	0.33	0.342	2.1	2.21
5	84.67	85.78	37.79	40.59	65.19	59.7	0.44	0.422	2.9	2.76
6	62.87	62.98	19.67	18.83	36.66	35.37	0.51	0.518	3.3	3.36
7	94.36	95.04	48.89	47.48	61.59	63.92	0.28	0.286	1.8	1.84
8	70.56	72.23	23.49	25.72	41.49	39.6	0.40	0.381	2.6	2.44
9	86.01	84.25	35.79	34.43	50.89	54.05	0.45	0.461	2.9	2.99

3.4. Multi-Response Optimization Using Grey Relation Analysis

3.4.1. Grey Relation Analysis Steps

Hard-turning is a multi-response process, and the relationship between the machining parameters and responses is intricate. Therefore, optimum machining parameters based on the multiple response variables can be determined using Grey Relation Analysis (GRA). Besides, the multi-response optimization drops to a single-response optimization using GRA [50,51]. Many researchers used GRA in their studies to optimize multiple responses [52–56]. The following steps should be performed for GRA:

Step 1: Normalization of response parameters

Since response parameter units are different (the cutting force components unit is "N" and the surface roughness unit is "μm"), all responses should be normalized to avoid different units and variability. Thus, all the response values were normalized between 0.00 and 1.00 based on their original values. In this case, the multi-responses can be compared with each other.

In the machining process, responses such as surface roughness and cutting forces are desired to be minimized; hence, the smaller-the-better characteristic is used for normalization considering Equation (11).

$$x_i^*(k) = \frac{\max x_i^0(k) - x_i^0(k)}{\max x_i^0(k) - \min x_i^0(k)} \tag{11}$$

where $i = 1, 2, \ldots, m$, and $k = 1, 2, \ldots, n$. m is the number of experimental data items, and n is the number of output parameters. $x_i^0(k)$ is the original sequence, $x_i^*(k)$ is the sequence after normalization, $\max x_i^0(k)$ is the highest value of $x_i^0(k)$, and $\min x_i^0(k)$ is the lowest value of $x_i^0(k)$.

However, some responses, such as tool life, should be maximized. Therefore, the higher-the-better is used to normalize the value using Equation (12).

$$x_i^*(k) = \frac{x_i^0(k) - \min x_i^0(k)}{\max x_i^0(k) - \min x_i^0(k)} \tag{12}$$

Step 2: Grey relation coefficient

Following the normalization, the grey relational coefficient is calculated to show the relationship between the ideal and actual normalized experimental results. Thus, the grey relational coefficient can be expressed mathematically as Equation (13),

$$\zeta_i(k) = \frac{\Delta_{\min} + \zeta\Delta_{\max}}{\Delta_{0i}(k) + \zeta\Delta_{\max}} \tag{13}$$

where, $\Delta_{0i}(k)$ is the deviation sequence of the reference sequence and the comparability sequence. $\Delta_{0i}(k)$ is calculated using Equation (14).

$$\Delta_{0i}(k) = \|x_0^*(k) - x_i^*(k)\| \tag{14}$$

where, $x_0^*(k)$ shows the reference sequence and $x_i^*(k)$ shows the comparability sequence. $\Delta_{\max}$ and $\Delta_{\min}$ are the maximum and minimum values of the absolute differences $\Delta_{0i}(k)$ of all comparing sequences. ζ is identification or distinguishing coefficient, which is in the range of 0 to 1. However, generally $\zeta = 0.5$ is used.

Step 3: Grey relation grades

According to Equation (15), the grey relational grade is calculated as the average of the grey relational coefficient.

$$\gamma_i = \frac{1}{n}\sum_{k=1}^{n} \zeta_i(k) \tag{15}$$

where, γ_i is the required grey relational grade for i_{th} test and n = number of outputs.

The multi-response optimization problem is converted into a single-response optimization problem employing the grey relational analysis-based Taguchi method [55–57]. The GRG shows the level of correlation between the reference sequence and the comparability sequence and is the total demonstrative of all the quality characteristics. Next, the mean grade relation grade is calculated for each level of the machining parameters. Thus, the optimum machining parameters are determined considering the maximum grey relational grade.

Step 4: ANOVA for GRG values

The Taguchi method could not be used to determine the machining parameters' effect on the multi-responses. Therefore, the ANOVA is performed on the GRG values at a 95% confidence level to determine the most significant factor in the multi-responses.

Step 5: Confirmation test

After determining the optimum machining parameters, it is needed to calculate the grey relation grade to predict and confirm the improvement of the performance factors. The grey relation grade prediction considering the optimum level of machining parameters is calculated using Equation (16).

$$\gamma_{predicted} = \gamma_m + \sum_{i=1}^{k} (\overline{\gamma}_i - \gamma_m) \tag{16}$$

where γ_m is the total mean GRG, $\overline{\gamma}_i$ is the mean GRG at the optimum level of each machining parameter, and k is the number of machining parameters that dominantly affect the multi-responses.

3.4.2. Implementation of Grey Relation Analysis

Firstly, experimental results are normalized for cutting force components and surface roughness using Equation (14). The normalized value for carbide and CBN inserts is given in Table 6.

Table 6. Normalized values for cutting forces and surface roughness.

Carbide Insert					
No	**Fx (N)**	**Fy (N)**	**Fz (N)**	**Ra (μm)**	**Rz (μm)**
1	1.000	1.000	1.000	0.679	0.650
2	0.789	0.648	0.747	0.393	0.400
3	0.535	0.368	0.417	0.000	0.000
4	0.551	0.497	0.580	0.857	0.850
5	0.281	0.182	0.217	0.500	0.450
6	0.822	0.914	0.850	0.179	0.150
7	0.000	0.000	0.000	1.000	1.000
8	0.653	0.791	0.690	0.643	0.650
9	0.300	0.318	0.382	0.393	0.400
CBN Insert					
No	**Fx (N)**	**Fy (N)**	**Fz (N)**	**Ra (μm)**	**Rz (μm)**
1	1.000	1.000	1.000	0.645	0.600
2	0.789	0.684	0.764	0.419	0.400
3	0.536	0.421	0.430	0.000	0.000
4	0.471	0.479	0.562	0.839	0.850
5	0.250	0.328	0.000	0.484	0.450
6	0.812	0.864	0.822	0.258	0.250
7	0.000	0.000	0.104	1.000	1.000
8	0.614	0.751	0.683	0.613	0.600
9	0.215	0.388	0.412	0.452	0.450

Secondly, after computing the deviation sequence, grey relational coefficients are calculated employing Equation (15) using 0.5 for the identification coefficient (ζ) based on the normalized values presented in Table 6. Finally, grey relational grade (GRG) is computed from the results of grey relational coefficients using Equation (15). The grey relation coefficient, grade, and the order for optimum machining parameters considering multi-responses are presented in Table 7.

Based on the ANOVA results, the feed rate is the dominant factor in the surface quality, and the cutting depth is the primary parameter of the cutting force components. The mean grey relation grades are calculated and presented in Table 8 for both cutting inserts. The maximum value of the mean GRG means the minimum cutting force components and surface roughness. As indicated in Table 8, the combination of V1-f1-a1-r2 machining parameters (V = 120 m/min, f = 0.04 mm/rev, a = 0.06 mm, r = 0.8 mm) is selected as the optimum machining parameters in both cutting inserts for the multiple-responses considering the highest mean grey relation grade, which indicates a stronger correlation to the reference sequence and better performance. The difference between the maximum and minimum GRG shows the contribution effect of the machining parameter on the multiple responses; a higher difference means a higher impact. According to Table 8, for carbide and CBN inserts, cutting depth has the dominant effect on the multiple responses, followed by feed rate. The cutting speed and nose radius have a negligible effect on the multi-responses. The main effects plot for the mean grey relation grade is depicted in Figure 6. The red squares show the optimum machining parameter levels for minimizing the multiple responses.

ANOVA results for the GRG value are presented in Table 9. According to the results, cutting depth is the most influential parameter in the multi-responses. It has a 46.93% and 43.36% contribution effect on the carbide and CBN inserts, respectively. It was followed by feed rate, with 40.37% and 40.18% contribution effects, respectively.

Table 7. Grey relation coefficient, grey relation grade, and the order for multi-responses.

Carbide Insert							
	Grey Relation Coefficient					**GRG**	**Order**
No	**Fx (N)**	**Fy (N)**	**Fz (N)**	**Ra (μm)**	**Rz (μm)**		
1	1.000	1.000	1.000	0.609	0.588	0.699	**1**
2	0.703	0.587	0.664	0.452	0.455	0.477	6
3	0.518	0.442	0.462	0.333	0.333	0.348	9
4	0.527	0.498	0.544	0.778	0.769	0.519	2
5	0.410	0.379	0.390	0.500	0.476	0.359	8
6	0.737	0.853	0.770	0.378	0.370	0.518	3
7	0.333	0.333	0.333	1.000	1.000	0.500	5
8	0.590	0.705	0.617	0.583	0.588	0.514	4
9	0.417	0.423	0.447	0.452	0.455	0.366	7
CBN Insert							
	Grey relation coefficient					**GRG**	**Order**
No	**Fx (N)**	**Fy (N)**	**Fz (N)**	**Ra (μm)**	**Rz (μm)**		
1	1.000	1.000	1.000	0.585	0.556	0.690	**1**
2	0.703	0.613	0.679	0.463	0.455	0.485	6
3	0.519	0.463	0.467	0.333	0.333	0.353	9
4	0.486	0.490	0.533	0.756	0.769	0.506	3
5	0.400	0.427	0.333	0.492	0.476	0.355	8
6	0.727	0.787	0.738	0.403	0.400	0.509	2
7	0.333	0.333	0.358	1.000	1.000	0.504	4
8	0.564	0.668	0.612	0.564	0.556	0.494	5
9	0.389	0.449	0.460	0.477	0.476	0.375	7

Table 8. Mean grey relation grade for carbide and CBN inserts.

Carbide Insert					
Cutting Parameters	Mean GRG			Max and Min Difference	Order
	Level 1	Level 2	Level 3		
V	**0.508**	0.465	0.460	0.048	3
f	**0.573**	0.450	0.411	0.162	2
a	**0.577**	0.454	0.402	0.175	**1**
r	0.475	**0.498**	0.460	0.038	4
Total Mean GRG: **0.478**					
CBN Insert					
Cutting Parameters	Mean GRG			Max and Min Difference	Order
	Level 1	Level 2	Level 3		
V	**0.509**	0.457	0.458	0.052	3
f	**0.567**	0.445	0.412	0.155	2
a	**0.564**	0.455	0.404	0.160	**1**
r	0.473	**0.499**	0.451	0.048	4
Total Mean GRG: **0.475**					

Table 9. ANOVA results for carbide and CBN inserts considering GRG values.

Carbide Inserts							
Source	**DF**	**Seq SS**	**Adj SS**	**Adj MS**	**F-Value**	***p*-Value**	**Cont.**
V	1	0.003456	0.003456	0.003456	1.60	0.274	3.54%
f	1	0.039366	0.039366	0.039366	18.28	0.013	**40.37%**
a	1	0.045763	0.045763	0.045763	21.25	0.010	**46.93%**
r	1	0.000308	0.000308	0.000308	0.14	0.724	0.32%
Error	4	0.008615	0.008615	0.002154			8.83%
Total	8	0.097508					100.00%
CBN Insert							
V	1	0.004004	0.004004	0.004004	1.62	0.272	4.50%
f	1	0.035728	0.035728	0.035728	14.46	0.019	**40.18%**
a	1	0.038560	0.038560	0.038560	15.60	0.017	**43.36%**
r	1	0.000748	0.000748	0.000748	0.30	0.611	0.84%
Error	4	0.009886	0.009886	0.002471			11.12%
Total	8	0.088926					100.00%

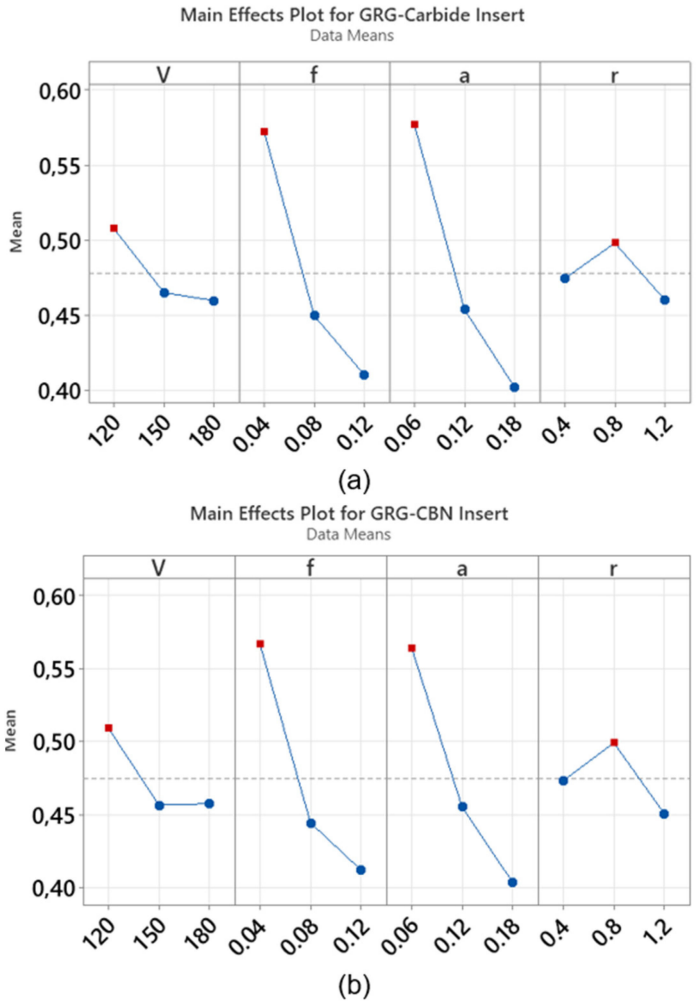

Figure 6. Main effects plots for mean grey relation grade (**a**) carbide insert, (**b**) CBN insert.

According to Equation (16), the predicted grey relation grades are determined using the optimum machining parameters. Table 10 compares the experimental results and the predicted GRG for optimum machining parameters. Based on the results, the cutting force components and surface roughness drop significantly for both cutting inserts using optimum machining parameters. Therefore, considering the initial and optimum machining parameters, an improvement of 0.477 (55.55%) and 0.485 (53.60%) was obtained in GRG for carbide and CBN inserts, respectively. These results are close to those obtained in previous studies [58–60]. Ranganathan and Senthilvelan [53] used the Taguchi-based GRA in the hot turning of stainless steel (type 316), increasing the GRG by 29.7%. Sarıkaya et al. [58] also used Taguchi-based GRA, which improved GRG by 39.4% in turning Haynes 25 alloy. In another study by Sarıkaya et al. [59], Taguchi-based GRA is used in turning AISI 1050 steel, which augments the GRG by 42.9%, considering the optimal machining parameters. Sahoo et al. [60] reported an improvement of 54.5% in GRG from the first machining parameter combination to the optimal machining parameter combination. Pekşen and Kalyon [61] also used Taguchi-based GRA in turning AISI 430 stainless steel, which enhanced the GRG by 69.1%. According to the literature study, multiple-response performance can be significantly increased by using Taguchi-based grey relation analysis in machining hard-to-cut materials.

Table 10. Confirmation test results.

Carbide Insert			
Initial Machining Parameters		**Optimum Machining Parameters**	
		Prediction	**Experiment**
Level	V_1 f_2 a_2 r_2	V_1 f_1 a_1 r_2	V_1 f_1 a_1 r_2
Fx	129.79		100.1
Fy	42.98		19.5
Fz	55.49		33.3
Ra	0.52		0.40
Rz	3.6		2.8
GRG	0.477	0.722	**0.742**
GRG improvement: **0.265** GRG improvement percentage: **55.55%**			
CBN Insert			
Initial machining parameters		**Optimum machining parameters**	
		Prediction	**Experiment**
Level	V_1 f_2 a_2 r_2	V_1 f_1 a_1 r_2	V_1 f_1 a_1 r_2
Fx	63.78		49.7
Fy	25.76		12.2
Fz	38.69		23.9
Ra	0.46		0.33
Rz	3.0		2.2
GRG	0.485	0.714	**0.745**
GRG improvement: **0.260** GRG improvement percentage: **53.60%**			

4. Conclusions

This study investigated the effects of machining parameters and tool geometry on surface roughness and cutting force components in dry hard-turning of AISI 4140 steel. In addition, the performance of coated carbide and CBN inserts was compared. The Taguchi method was used for the design of the experiment; ANOVA was used to determine the contribution effect of independent variables on the dependent variables; and multi-response optimization of the grey relation analysis was utilized to determine the optimum machining parameters for each insert. The findings of the current study are presented below:

- For coated carbide and CBN inserts, Ra was measured in the range of 0.35–0.63 μm and 0.28–0.59 μm, respectively. Besides, for coated carbide and CBN inserts, Rz was measured in the range of 2.4–4.4 μm and 1.8–3.8 μm, respectively. The best surface quality was obtained using a CBN insert (0.28 μm) with a combination of high cutting speed (180 m/min) and low feed rate (0.04 mm/rev). The feed rate is a function of the chip's cross-sectional area. Therefore, by increasing the feed rate, the chip area rises, which results in higher surface roughness. As the cutting speed increases, the built-up edge (BUE) on the cutting tool is reduced, which leads to better surface quality.
- Feed rate was a dominant factor on both Ra and Rz for both cutting inserts. The contribution effect of feed rate on the Ra for carbide and CBN inserts was 80% and 73.76%, respectively. It was followed by cutting speed with 19.28% and 23.43% contribution effects, respectively. Increasing the feed rate value significantly increases the surface roughness components (Ra and Rz). On the contrary, increasing the cutting speed decreases the surface roughness. The undeformed chip thickness increases as the feed rate rises, resulting in high surface roughness. CBN inserts exhibited 14% better performance than carbide inserts in terms of surface quality.
- The cutting force components for carbide and CBN inserts are 25.06–198.56 N and 15.09–94.36 N, respectively. The cutting force components in CBN inserts are lower than

in carbide inserts. CBN inserts exhibited 103%, 62%, and 40% better performance than carbide inserts in terms of Fx, Fy, and Fz, respectively. Cutting depth was the dominant factor in all cutting force components. As the cutting depth increases, the Fx, Fy, and Fz augment sharply. Cutting speed is the next important factor in cutting forces. Increasing the cutting speed increases the cutting forces as well. Therefore, a combination of low cutting speed and cutting depth is needed to reduce the cutting forces.

- The developed models can predict the response with very good accuracy, and the graphical comparison of the predicted and experimental results shows perfect agreement between the results.
- The Taguchi-based grey relation analysis was performed to determine the optimum machining parameters. The cutting depth and feed rate have a dominant effect on the multi-responses. The contribution effect of cutting depth on the multi-responses for carbide and CBN inserts is 46.93% and 43.36%, respectively. Besides, the feed rate has a 40.37% and 40.18% contribution effect, respectively. Based on the obtained grey relation grade, a combination of 120 m/min cutting speed, 0.04 mm/rev feed rate, 0.06 mm cutting depth, and 0.8 mm nose radius should be selected for multi-response optimization.

Author Contributions: Conceptualization: M.R. and M.Ö.; Investigation: M.R., M.Ö. and M.A.A.; Experimental Test: M.Ö.; Methodology: M.R. and M.Ö., Software: M.R.; Validation: M.R.; Manuscript draft preparation: M.R., M.Ö. and M.A.A.; Visualization: M.R. and M.Ö.; Paper writing, review, and editing: M.R., M.Ö. and M.A.A. All authors have read and agreed to the published version of the manuscript.

Funding: 1. The author extends their appreciation to the Deanship of Scientific Research, the King Khalid University of Saudi Arabia, for funding this work through the Large Groups Research Project under grant number (RGP.2/163/43). 2. This research was funded by Yozgat Bozok Üniversitesi Bilimsel Araştırmalar Projeleri (BAP), Project No: 6601-FBE/20-352.

Institutional Review Board Statement: Not applicable.

Informed Consent Statement: Not applicable.

Data Availability Statement: Not applicable.

Conflicts of Interest: The authors declare no conflict of interest.

References

1. Awasthi, A.; Saxena, K.K.; Arun, V. Sustainable and smart metal forming manufacturing process. *Mater. Today Proc.* **2021**, *44*, 2069–2079. [CrossRef]
2. Das, A.; Patel, S.K.; Hotta, T.K.; Biswal, B.B. Statistical analysis of different machining characteristics of EN-24 alloy steel during dry hard turning with multilayer coated cermet inserts. *Measurement* **2019**, *134*, 123–141. [CrossRef]
3. Tönshoff, H.; Arendt, C.; Amor, R.B. Cutting of hardened steel. *CIRP Ann.* **2000**, *49*, 547–566. [CrossRef]
4. Klocke, F.; Brinksmeier, E.; Weinert, K. Capability profile of hard cutting and grinding processes. *CIRP Ann.* **2005**, *54*, 22–45. [CrossRef]
5. Chinchanikar, S.; Choudhury, S. Machining of hardened steel—Experimental investigations, performance modeling and cooling techniques: A review. *Int. J. Mach. Tools Manuf.* **2015**, *89*, 95–109. [CrossRef]
6. Chinchanikar, S.; Choudhury, S. Effect of work material hardness and cutting parameters on performance of coated carbide tool when turning hardened steel: An optimization approach. *Measurement* **2013**, *46*, 1572–1584. [CrossRef]
7. Panda, A.; Das, S.R.; Dhupal, D. Surface roughness analysis for economical feasibility study of coated ceramic tool in hard turning operation. *Process Integr. Optim. Sustain.* **2017**, *1*, 237–249. [CrossRef]
8. Das, R.K.; Kumar, R.; Sarkar, G.; Sahoo, S.; Sahoo, A.K.; Mishra, P.C. Comparative machining performance of hardened AISI 4340 Steel under dry and minimum quantity lubrication environments. *Mater. Today Proc.* **2018**, *5*, 24898–24906. [CrossRef]
9. Gürbüz, H.; Emre Gönülaçar, Y. Optimization and evaluation of dry and minimum quantity lubricating methods on machinability of AISI 4140 using Taguchi design and ANOVA. *Proc. Inst. Mech. Eng. Part C J. Mech. Eng. Sci.* **2021**, *235*, 1211–1227. [CrossRef]
10. Chou, Y.K.; Evans, C.J. Tool wear mechanism in continuous cutting of hardened tool steels. *Wear* **1997**, *212*, 59–65. [CrossRef]
11. Rastorguev, D.; Sevastyanov, A. Diagnostics of chip formation and surface quality by parameters of the main drive current in the hard turning. *Mater. Today Proc.* **2019**, *19*, 1845–1851. [CrossRef]
12. He, K.; Gao, M.; Zhao, Z. Soft computing techniques for surface roughness prediction in hard turning: A literature review. *IEEE Access* **2019**, *7*, 89556–89569. [CrossRef]
13. Tzotzis, A.; García-Hernández, C.; Huertas-Talón, J.L.; Kyratsis, P. Influence of the nose radius on the machining forces induced during AISI-4140 hard turning: A CAD-based and 3D FEM approach. *Micromachines* **2020**, *11*, 798. [CrossRef] [PubMed]

14. Schwalm, J.; Gerstenmeyer, M.; Zanger, F.; Schulze, V. Complementary Machining: Effect of tool types on tool wear and surface integrity of AISI 4140. *Procedia CIRP* **2020**, *87*, 89–94. [CrossRef]
15. Dogra, M.; Sharma, V.; Dureja, J. Effect of tool geometry variation on finish turning—A Review. *J. Eng. Sci. Technol. Rev.* **2011**, *4*, 1–13. [CrossRef]
16. Nikam, B.; Khadtare, A.; Pawade, R. Machinability Assesment of AISI 4140 Hardened Steel Using CBN Inserts in Hard Turning. *Int. J. Mod. Manuf. Technol.* **2021**, *13*, 140–148.
17. Aouici, H.; Elbah, M.; Yallese, M.A.; Fnides, B.; Meddour, I.; Benlahmidi, S. Performance comparison of wiper and conventional ceramic inserts in hard turning of AISI 4140 steel: Analysis of machining forces and flank wear. *Int. J. Adv. Manuf. Technol.* **2016**, *87*, 2221–2244. [CrossRef]
18. Das, S.R.; Dhupal, D.; Kumar, A. Experimental investigation into machinability of hardened AISI 4140 steel using TiN coated ceramic tool. *Measurement* **2015**, *62*, 108–126. [CrossRef]
19. Şahinoğlu, A.; Rafighi, M. Investigation of vibration, sound intensity, machine current and surface roughness values of AISI 4140 during machining on the lathe. *Arab. J. Sci. Eng.* **2020**, *45*, 765–778. [CrossRef]
20. Iynen, O.; Şahinoğlu, A.; Özdemir, M.; Yilmaz, V. Investigation of the effect of cutting parameters on the surface roughness value in the machining of AISI 4140 steel with Taquchi method. *J. Inst. Sci. Technol.* **2020**, *10*, 2840–2849. [CrossRef]
21. Upadhyay, V.V. Machining parameters optimization by grey relational analysis of alloy steel AISI 4140. *PalArch's J. Archaeol. Egypt/Egyptol.* **2020**, *17*, 4107–4121.
22. Elbah, M.; Laouici, H.; Benlahmidi, S.; Nouioua, M.; Yallese, M.A. Comparative assessment of machining environments (dry, wet and MQL) in hard turning of AISI 4140 steel with CC6050 tools. *Int. J. Adv. Manuf. Technol.* **2019**, *105*, 2581–2597. [CrossRef]
23. Tiwari, A.; Makhesana, M.A.; Patel, K.M.; Mawandiya, B.K. Experimental investigations on the applicability of solid lubricants in processing of AISI 4140 steel. *Mater. Today Proc.* **2020**, *26*, 2921–2925. [CrossRef]
24. Sultana, M.; Zaman, P.B.; Dhar, N.R. GRA-PCA coupled with Taguchi for optimization of inputs in turning under cryogenic cooling for AISI 4140 steel. *J. Prod. Syst. Manuf. Sci.* **2020**, *1*, 40–62.
25. Nicolodi, J.H.W.; Consalter, L.A.; Durán, O.; Souza, A.J. Effect of wear progression in an 'S'-type mixed ceramic tool on machining forces and surface roughness in the turning of hardened AISI 4140 steel. *Int. J. Mach. Mach. Mater.* **2019**, *21*, 228–243. [CrossRef]
26. Meddour, I.; Yallese, M.A.; Bensouilah, H.; Khellaf, A.; Elbah, M. Prediction of surface roughness and cutting forces using RSM, ANN, and NSGA-II in finish turning of AISI 4140 hardened steel with mixed ceramic tool. *Int. J. Adv. Manuf. Technol.* **2018**, *97*, 1931–1949. [CrossRef]
27. Zahia, H.; Athmane, Y.; Lakhdar, B.; Tarek, M. On the application of response surface methodology for predicting and optimizing surface roughness and cutting forces in hard turning by PVD coated insert. *Int. J. Ind. Eng. Comput.* **2015**, *6*, 267–284. [CrossRef]
28. Paengchit, P.; Saikaew, C. Effects of Cutting Speed and Feed Rate on Surface Roughness in Hard Turning of AISI 4140 with Mixed Ceramic Cutting Tool. *Key Eng. Mater.* **2018**, *79*, 153–158. [CrossRef]
29. Rafighi, M.; Özdemir, M.; Das, A.; Das, S.R. Machinability investigation of cryogenically treated hardened AISI 4140 alloy steel using CBN insert under sustainable finish dry hard turning. *Surf. Rev. Lett.* **2022**, *29*, 2250047. [CrossRef]
30. Sahinoglu, A.; Rafighi, M. Machinability of hardened AISI S1 cold work tool steel using cubic boron nitride. *Sci. Iran.* **2021**, *28*, 2655–2670. [CrossRef]
31. Rafighi, M. Effects of shallow cryogenic treatment on surface characteristics and machinability factors in hard turning of AISI 4140 steel. *Proc. Inst. Mech. Eng. Part E J. Process Mech. Eng.* **2022**, *236*, 2118–2130. [CrossRef]
32. Akkuş, H. Experimental and Statistical Investigation of Surface Roughness in Turning of AISI 4140 Steel. *Sak. Univ. J. Sci.* **2019**, *23*, 775–781. [CrossRef]
33. Bagal, D.K.; Parida, B.; Barua, A.; Jeet, S.; Sahoo, B.B. Multi-parametric optimization in CNC dry turning of chromoly steel using taguchi coupled desirability function analysis and utility concept. *Int. J. Appl. Eng. Res* **2019**, *14*, 21–26.
34. Aouad, R.; Amara, I. Influence of the cutting condition on the wear and the surface roughness in the steel AISI 4140 with mixed ceramic and diamond tool. *J. Eng. Des. Technol.* **2018**, *16*, 828–836. [CrossRef]
35. Şahinoğlu, A.; Ulas, E. An investigation of cutting parameters effect on sound level, surface roughness, and power consumption during machining of hardened AISI 4140. *Mech. Ind.* **2020**, *21*, 523. [CrossRef]
36. Karaaslan, F.; Şahinoğlu, A. Determination of ideal cutting conditions for maximum surface quality and minimum power consumption during hard turning of AISI 4140 steel using TOPSIS method based on fuzzy distance. *Arab. J. Sci. Eng.* **2020**, *45*, 9145–9157. [CrossRef]
37. Rajeev, D.; Dinakaran, D.; Singh, S. Artificial neural network based tool wear estimation on dry hard turning processes of AISI4140 steel using coated carbide tool. *Bull. Pol. Acad. Sci. Tech. Sci.* **2017**, *65*, 553–559. [CrossRef]
38. Sahoo, S. Review on Hard Turning using Finite Element Method. *J. Eng. Innov. Res.* **2019**, *9*, 61–68.
39. Boing, D.; Zilli, L.; Fries, C.E.; Schroeter, R.B. Tool wear rate of the PCBN, mixed ceramic, and coated cemented carbide in the hard turning of the AISI 52100 steel. *Int. J. Adv. Manuf. Technol.* **2019**, *104*, 4697–4704. [CrossRef]
40. Anand, A.; Behera, A.K.; Das, S.R. An overview on economic machining of hardened steels by hard turning and its process variables. *Manuf. Rev.* **2019**, *6*, 4. [CrossRef]
41. Mir, M.J.; Wani, M.F.; Banday, S.; Mushtaq, S.; Khan, J.; Singh, J.; Saleem, S.S. Comparative assessment of coated CBN and multi-layer coated carbide tools on tool wear in hard turning AISID2 steel. In Proceedings of the TRIBOINDIA-2018 an International Conference on Tribology, Maharashtra, India, 13–15 December 2018.

42. Szwajka, K.; Zielińska-Szwajka, J.; Trzepiecinski, T. Experimental study on drilling MDF with tools coated with TiAlN and ZrN. *Materials* **2019**, *12*, 386. [CrossRef] [PubMed]
43. Gadelmawla, E.S.; Koura, M.M.; Maksoud, T.M.; Elewa, I.M.; Soliman, H.H. Roughness parameters. *J. Mater. Process. Technol.* **2002**, *123*, 133–145. [CrossRef]
44. Panda, A.; Das, S.R.; Dhupal, D. Statistical Analysis of Surface Roughness Using RSM in Hard Turning of AISI 4340 Steel with Ceramic Tool. In *Advances in Industrial and Production Engineering*; Springer: Singapore, 2019; pp. 17–26.
45. Sadik, M.I. Wear development and cutting forces on CBN cutting tool in hard part turning of different hardened steels. *Procedia CIRP* **2012**, *1*, 232–237. [CrossRef]
46. Iynen, O.; Şahinoğlu, A.; Özdemir, M.; Yilmaz, V. Optimization of the effect of cutting parameters on the cutting force in the gradual turning process by Taguchi method. *J. Inst. Sci. Technol.* **2020**, *10*, 1909–1918. [CrossRef]
47. Tzotzis, A.; Garcia-Hernandez, C.; Huertas-Talon, J.L.; Kyratsis, P. 3D FE Modelling of Machining Forces during AISI 4140 Hard Turning. *Stroj. Vestn./J. Mech. Eng.* **2020**, *66*, 467–478. [CrossRef]
48. Mohd, A.; Mohd, A.; Adnan, M.H.; Baba, N.B.; Selamat, Z.A.; Rose, A.N.; Mohamed, S.B. Optimization of surface roughness and tool wear on AISI 4140 using coated Ni-YSZ for CNC turning process. *J. Phys. Conf. Ser.* **2020**, *1532*, 012001. [CrossRef]
49. Szwajka, K.; Trzepieciński, T. An examination of the tool life and surface quality during drilling melamine faced chipboard. *Wood Res.* **2017**, *62*, 307–318.
50. Julong, D. Introduction to grey system theory. *J. Grey Syst.* **1989**, *1*, 1–24.
51. Elsayed, E.; Chen, A. Optimal levels of process parameters for products with multiple characteristics. *Int. J. Prod. Res.* **1993**, *31*, 1117–1132. [CrossRef]
52. Pan, L.K.; Wang, C.C.; Wei, S.L.; Sher, H.F. Optimizing multiple quality characteristics via Taguchi method-based Grey analysis. *J. Mater. Process. Technol.* **2007**, *182*, 107–116. [CrossRef]
53. Ranganathan, S.; Senthilvelan, T. Multi-response optimization of machining parameters in hot turning using grey analysis. *Int. J. Adv. Manuf. Technol.* **2011**, *56*, 455–462. [CrossRef]
54. Vinayagamoorthy, R.; Xavior, M.A. Parametric optimization on multi-objective precision turning using grey relational analysis. *Procedia Eng.* **2014**, *97*, 299–307. [CrossRef]
55. Panda, A.; Sahoo, A.; Rout, R. Multi-attribute decision making parametric optimization and modeling in hard turning using ceramic insert through grey relational analysis: A case study. *Decis. Sci. Lett.* **2016**, *5*, 581–592. [CrossRef]
56. Sivaiah, P.; Chakradhar, D. Multi performance characteristics optimization in cryogenic turning of 17-4 PH stainless steel using Taguchi coupled grey relational analysis. *Adv. Mater. Process. Technol.* **2018**, *4*, 431–447. [CrossRef]
57. Senthilkumar, N.; Tamizharasan, T.; Anandakrishnan, V. Experimental investigation and performance analysis of cemented carbide inserts of different geometries using Taguchi based grey relational analysis. *Measurement* **2014**, *58*, 520–536. [CrossRef]
58. Sarıkaya, M.; Güllü, A. Multi-response optimization of minimum quantity lubrication parameters using Taguchi-based grey relational analysis in turning of difficult-to-cut alloy Haynes 25. *J. Clean. Prod.* **2015**, *91*, 347–357. [CrossRef]
59. Sarıkaya, M.; Yılmaz, V.; Dilipak, H. Modeling and multi-response optimization of milling characteristics based on Taguchi and gray relational analysis. *Proc. Inst. Mech. Eng. Part B J. Eng. Manuf.* **2016**, *230*, 1049–1065. [CrossRef]
60. Sahoo, A.K.; Sahoo, B. Performance studies of multilayer hard surface coatings (TiN/TiCN/Al_2O_3/TiN) of indexable carbide inserts in hard machining: Part-II (RSM, grey relational and techno economical approach). *Measurement* **2013**, *46*, 2868–2884. [CrossRef]
61. Pekşen, H.; Kalyon, A. Optimization and measurement of flank wear and surface roughness via Taguchi based grey relational analysis. *Mater. Manuf. Process.* **2021**, *36*, 1865–1874. [CrossRef]